EPJ Web of Conferences **169**, 00026 (2018) https://doi.org/10.1051/epjconf/201816900026
Theory-4

Measurement of the prompt fission γ-ray spectrum of ^{242}Pu

Sebastian Urlass[1,2,⋆], *Roland* Beyer[1], *Arnd Rudolf* Junghans[1,⋆⋆], *Toni* Kögler[1], *Ronald* Schwengner[1], and *Andreas* Wagner[1]

[1] *Helmholtz-Zentrum Dresden-Rossendorf, Bautzener Landstraße 400, 01328 Dresden, Germany*
[2] *Technische Universität Dresden, 01062 Dresden, Germany*

Abstract. The prompt γ-ray spectrum of fission fragments is important in understanding the dynamics of the fission process, as well as for nuclear engineering in terms of predicting the γ-ray heating in nuclear reactors. The γ-ray spectrum measured from the fission fragments of the spontaneous fission of ^{242}Pu will be presented here. A fission chamber containing in total 37 mg of ^{242}Pu was used as active sample. The γ-quanta were detected with high time- and energy-resolution using $LaBr_3$ and HPGe detectors, respectively, in coincidence with spontaneous fission events detected by the fission chamber. The acquired γ-ray spectra were corrected for the detector response using the spectrum stripping method. About 70 million fission events were detected which results in a very low statistical uncertainty and a wider energy range covered compared to previous measurements. The prompt fission γ-ray spectrum measured with the HPGe detectors shows structures that allow conclusions about the nature of γ-ray transitions in the fission fragments. The average photon multiplicity of 8.2 and the average total energy release by prompt photons per fission event of about 6.8 MeV were determined for both detector types.

1 Introduction

The emission of γ-quanta after nuclear fission plays an important role for the design of future nuclear power plants. The local contribution of the heat generation from γ-rays has to be known very accurately to develop an efficient core-design. Therefore the prompt and delayed γ-emission spectra from the nuclear fission process must be known. In recent years several integral experiments showed discrepancies with simulations up to 30% [1]. For that reason the neutron induced fission prompt γ-ray spectrum (PFGS) for the reactor fuels ^{239}Pu and ^{235}U were taken into the High Priority Request List of the OECD / Nuclear Energy Agency [2].

For future transmutation technologies also the understanding of the burn-up of minor actinides like the longlived ^{242}Pu is from interest. Beside the technological aspect the measurement of the PFGS from spontaneous fission (SF) of ^{242}Pu and the determination of its characteristics is also important for a general parameterization of fission observables. These characteristics are the average energy release $\overline{\epsilon}_\gamma$, the average total energy release $\overline{E}_\gamma$ and average photon multiplicity $\overline{\nu}_\gamma$ per fission. In order

⋆ Corresponding author, e-mail: s.urlass@hzdr.de
⋆⋆ Principal corresponding author, e-mail: a.junghans@hzdr.de

to separate prompt and delayed γ-rays from fission $LaBr_3$ detectors with a good time resolution are used.

Another aspect for this experiment is the investigation of the dynamics of the fission process. Most fission fragments (FF) are neutron rich nuclei with an initial excitation energy above the neutron separation energy, so that at first prompt neutrons are emitted. A high angular momentum neutron emission is surppressed due to the angular momentum barrier. That means it does not affect the angular momenta of the fission fragments very strongly. If the excitation energy is below the neutron separation energy, prompt γ-ray emission takes place. At a certain point of the deexcitation, when the Yrast-line is reached, the fission fragments are in a collective rotational state. The remaining high angular momentum of the FF can be carried away via electrical quadrupole transitions (E2) [3]. To be able to resolve transitions from known rotational bands in FF, high purity germanium detectors with a high energy resolution were used.

2 Setup, data acquisition and measurement

For the detection of FF a parallel plate fission ionization chamber was used. All details about the PuFC can be found in Ref. [4, 5]. In the following only the most crucial properties the PuFC regarding the PFGS measurement are presented. The PuFC consists of 8 pairs of electrodes, which are disks of 98 mm diameter, mounted with a gap of 10 mm between each other. The cathodes are silicon wafers of 400 µm thickness where the ^{242}Pu was deposited as circular layers of 74 mm diameter using the molecular plating technique [6]. The plutonium content of each deposit is listed in Table 1. In total the fission chamber contains 37.2 mg plutonium.

Table 1. Properties of Pu deposits. The left table a) contains the isotopic vector, which was determined by using mass spectroscopy. The mass of each Pu deposit is shown in the right table b). These quantities were obtained from the SF-rate of ^{242}Pu [4].

a) isotope vector

isotope	mass fraction/%
^{238}Pu	0.002
^{239}Pu	0.005
^{240}Pu	0.022
^{241}Pu	0.002
^{242}Pu	99.967
^{244}Pu	0.002

b) deposit mass

Pu deposit	mass/mg
# 1	5.42 (9)
# 2	4.89 (8)
# 3	4.37 (7)
# 4	4.22 (7)
# 5	4.44 (7)
# 6	4.43 (7)
# 7	4.13 (7)
# 8	5.33 (9)
sum	37.24 (22)

The anodes consist of tantalum with a thickness of 100 µm. Due to safety- and radiation protection reasons the housing material is made of 3 mm thick stainless steel, with exception of the front- and end window which are made of 200 µm thick stainless steel foil. P10 (90% Argon+10% Methane) is used as counting gas. The total SF-rate in the chamber is about 30 fission events per second, while its corresponding α-activity is about 8 MBq. The quality of the separation of both contributions can be seen in the charge specrum of the first Pu deposit which is depicted in Fig. 1.

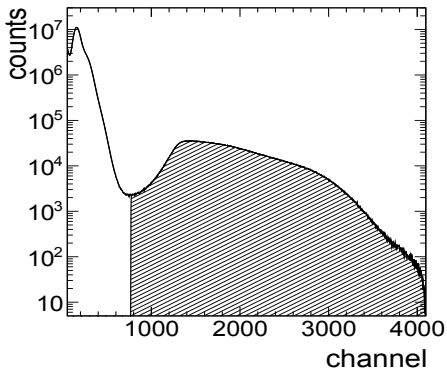

Figure 1. Measured charge spectrum of the first Pu deposit. The charge spectra of the other deposits have a similar spectral shape and are not depicted due to overview reasons. At the channel position of about 800 is a local minimum of the spectrum. Below the minimum the charge spectrum is dominated by α-particles. The induced charge spectrum above the minimum consists of contributions from FF, pile-up of FF with each other and α-particles. The latter one and also multiple pile-up of α-particles with each other is negligible. In order to create the correlation between fission event and γ-ray emission a gate was set for all charge spectra in a way that the defined FF regions contain channel values greater than their corresponding local minima. This region is depicted here for the first deposit as hatched area.

The time resolution of the chamber is about 2 ns (FWHM) and its FF detection probability is nearly 100%. For reasons of pile-up reduction the readout of the Pu signals is done separately for each deposit. These signals are amplified with charge sensitive fast preamplifiers (CSP) which were developed at HZDR. Figure 2 illustrates the entire setup of the experiment and its corresponding electrical scheme.

Two different types of detecors were used to measure the photons in coincidence with a detected fission fragment. These are named in the following as γ-ray detector. As the first type of γ-ray detector three 7.62 cm $\times$ 7.62 cm (diameter $\times$ length) $LaBr_3$ detectors were used[1]. Their energy resolution[2] is about 4% and the time resolution is approximately 0.8 ns (FWHM). The second type of γ-ray detector are two high purity germanium (HPGe) cluster detectors of the MINIBALL design [7]. Each cluster consists of three capsules containing the HPGe crystal so that all together six HPGe detectors are used. Their energy resolution[2] is about 0.3% while the time resolution is about 10 ns (FWHM). Both time and energy information are measured by the data aquisition and stored in list mode. The triggerlogic of the experiment is based on a logical OR condition between all detectors and is controlled by an FPGA module, which means that each detector can trigger the data acquisition seperately. During the measurement all γ-ray detectors were affected by gain shifts. Recording at first all uncorrelated γ-events shows the advantage for applying a gain correction procedure with high statistics in a short amount of time, which is based on the time dependent shifts of peak positions from the natural background. The initializing and readout of all modules QDC, ADC and TDC is done by RIO4 power PC which communicates via a VME BUS. The RIO4 is operated with a Multibranching System (MBS) which is developed at GSI Darmstadt [8]. The MBS-list-mode data were analysed with the software package Go4 [9]. In the offline analysis a coincidence between PuFC and γ-ray detectors has been created. During the measurement time of about six weeks 70 million fission events were registered. Beside this

[1] Saint-Gobain *BrilLanCe 380 Scintillation Products Technical Note, Performance Summary* (2009).

[2] The energy resolution is here defined as relative quantity $\frac{\Delta E}{E}$ where ΔE corresponds to a measured FWHM at the energy E =1333 keV using a ^{60}Co calibration source.

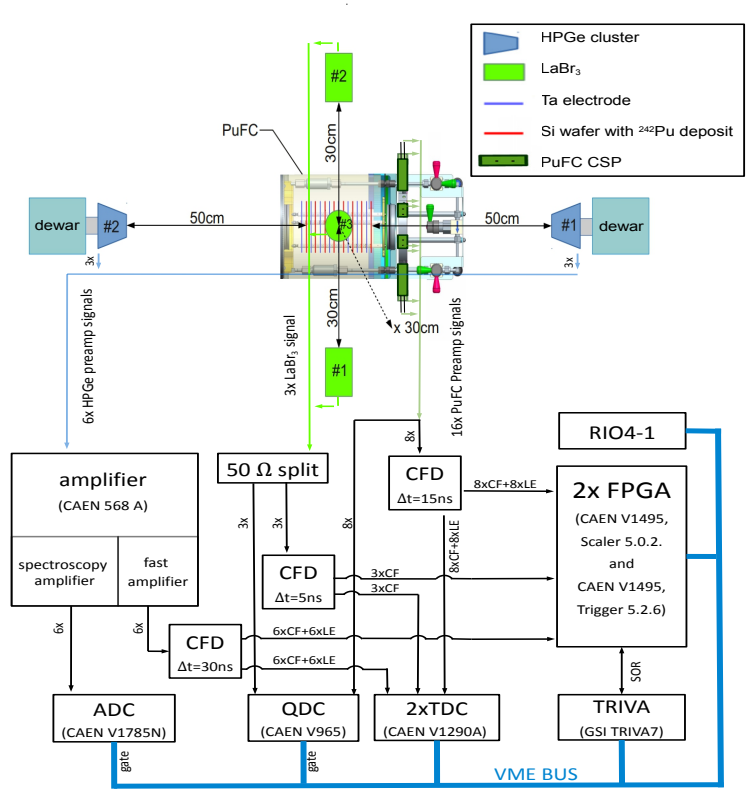

Figure 2. Sketch of experimental setup and electronics. The upper part shows the detector setup. The PuFC with its CSP is in the middle. Around the PuFC the three $LaBr_3$ detectors are placed perpendicular to the FC housing with a distance of 30cm to the center of the FC axis. One of the $LaBr_3$ detectors is mounted perpendicular above the plane of projection, illustrated as light green disk centered on the PuFC. The MINIBALL HPGe detectors are mounted in front of a stainless steel window of the PuFC. The distance between each of these cluster detectors from die closest PuFC deposit is 50cm. A simple scheme of the electronics is illustrated in the lower part. The time information is acquired by a time to digital converter (TDC). The match window for the event trigger for the TDC is $\pm 1\,\mu s$. The charge informations of the PuFC and the $LaBr_3$ signals are recorded by a charge to digital converter (QDC.) The amplitude informations from the HPGe detectors are recorded by an amplitude to digital converter (ADC).

long-term measurement a series of efficiency and energy calibrations with calibrated sources using an identical fission chamber without Pu deposits were performed.

3 Separation of prompt- and delayed γ-rays and Slow rise time correction

In order to get a proper determination of the timing of the signals, constant fraction discriminator (CFD) modules[3], with Amplitude-Risetime-Compensation (ARC) technique [10], are used. This

[3]Inhouse development of HZDR.

ARC-timing property is necessary for the HPGe detectors which have variable rise times because of the different charge collection time inside the HPGe crystal volume. A CFD splits the input signal in an inverted and delayed and an attenuated signal. The superposition of both signals creates a bipolar signal with a zero crossing which is independent from the signal amplitudes, if the rise times of all input signals are the same. To get also a rise time independent zero crossing, the delay Δt between the splitted signals that can be adjusted by an external cable delay were chosen very short compared to the signal rise times, for instance 5 to 30 ns (see Fig. 2). For the application of the ARC-timing, in case for the HPGe detectors, a price has to be paid. The CFD has an internal integrated arming threshold discriminator, which is necessary to prevent to trigger electronic noise. If the zero crossing time occurs before reaching the arming threshold, the discriminator will not be armed and the signal is not registered. This effect occurs very strongly for low amplitude values for the HPGe signals.

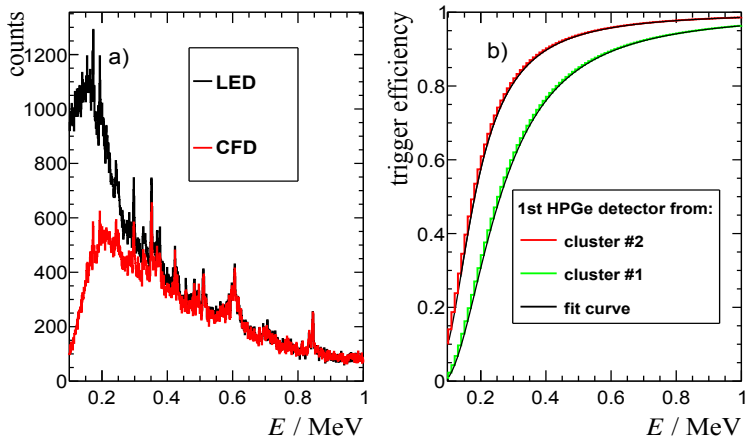

Figure 3. CFD-trigger efficiency for the HPGe detectors. In a) the lack of the CFD arming is illustrated for the first HPGe detector of the second cluster. The integral of the spectrum for CFD triggered events is about 40% less than in comparison to the LED spectrum. In b) the measured trigger efficiencies for the first HPGe detector of the first and second MINIBALL cluster, respectively, are shown with their corresponding fit curves described by Eq. (1). A strong decrease of the trigger efficiencies are visible for energies below 400 keV.

The increase of the delay leads to a better CFD-trigger behaviour but makes the time resolution much worse. The compromise to keep the good time resolution is applying an additional correction in the offline analysis for CFD triggered events at low energies. Therefore a leading edge threshold discriminator (LED) has been used as a reference. The LED is able to register all events with energies greater than 100 keV. The ratio of CFD- and LED triggered γ-ray events in coincidence with the PuFC gives a quantity for the lack of the CFD arming and is in the following named as trigger efficiency $\epsilon_{\mathrm{CFD}}(E)$, which is described by an empirical formula. This function for $\epsilon_{\mathrm{CFD}}(E)$ is shown in Eq. (1) and illustrated in Fig. 3b). In Fig. 3a) the difference between the CFD- and LED triggered amplitude spectra is illustrated.

$$\epsilon_{\mathrm{CFD}}(E) = 1 + \frac{1}{a_0 + a_1 \cdot E + a_2 \cdot E^2} \tag{1}$$

The application of ARC timing allows us to get a reasonable time resolution for all the HPGe detectors of about 12 ns in coincidence with the PuFC. The combined time resolution of the coincidence between the $LaBr_3$ detectors and the PuFC was measured to 2.3 ns. In Fig. 4 the energy spectra of both γ-detector types in coincidence with the PuFC are shown. In order to extract only the prompt fission γ-rays a gate for a coincidence window of $\Delta T = \pm 3$ ns for the $LaBr_3$ and $\Delta T = \pm 12$ ns for the

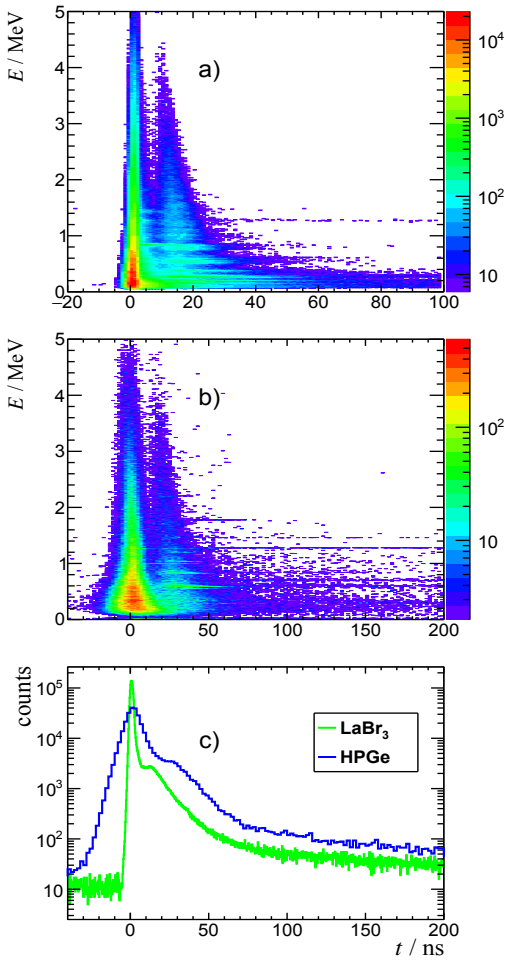

Figure 4. Energy spectra in correlation to prompt- and delayed γ-rays from the fission process. In a) the summed spectrum of all $LaBr_3$ detectors is illustrated. In b) the summed spectrum for all the HPGe detectors is shown. Note the different time scales for both detector types. The time t is calibrated in a way that the time of flight of the prompt γ-rays corresponds to a flight path of 30 cm for the $LaBr_3$ detectors and 50 cm for the HPGe detectors respectively. The time spectra of both γ-ray detector types, projected for all energies, are illustrated in c).

HPGe detectors was set. The delayed γ-rays appearing in this measurement can be categorized in four different contributions:

1. random events:
The γ-rays from the natural background appear randomly in the coincidence time window for the prompt photons and are time independent. Its strongest background contribution comes from ^{40}K (1461 keV) decay and an can be barely seen in Fig. 4b) as horizontal line.

2. (n, n′) on γ-detector material:
In Fig. 4c) the bump structure after the prompt events is due to the (n, n′) reactions, which time delay depends on the distance between the γ-detector and the PuFC. Most of the delayed γ-rays for the $LaBr_3$ detectors could be identified to stem from (n, n′) reactions with the detector material containing the major isotopes ^{139}La, ^{79}Br and ^{81}Br in an energy range of 160–800 keV and can be

seen in Fig. 3a) the difference between the CFD- and LED triggered amplitude spectra is illustrated. 4a) and c) about 10 ns after the prompt γ-rays. In case for the HPGe detectors (n, n′) reactions with the most abundant isotopes ^{70}Ge, ^{72}Ge, ^{74}Ge and ^{76}Ge could be identified in an energy range of 600–2000 keV and can be seen in Fig. 4b) and c) about 20 ns after the prompt γ-rays.

3. (n, n′) on the PuFC material:
The large amount of ^{56}Fe in the PuFC material leads to γ-rays with energies of 847 keV from the first excited state and appear due to the short deposit-to-PuFC housing flight path and its corresponding minimal neutron time of flight of 2 ns very close to the time of flight of prompt photons for the $LaBr_3$ detectors. Because of its good time resolution this contribution can be separated from the prompt γ-events. In case for the HPGe detectors (n, n′) reactions on ^{56}Fe can be barely distinguished from prompt γ-quanta but these reactions are also much less expected than for the $LaBr_3$ detectors. Most of the detected photons are emitted in longditudinal direction and pass mainly the 200 μm thick stainless steel windows.

4. Isomeric states from FF:
In this measurement the most significant delayed γ-ray contribution of this type can be identified from an isomeric 6^+ state at 1691 keV of the FF ^{134}Te with a lifetime of about 164 ns (see Ref. [11]). During its deexcitation process also the the short lived first excited 2^+ state (0.64 ps) at 1279 keV) is populated. This photon energy can be seen as horizontal line[4] in Fig. 4a) and b).

4 Response correction, results and discussion

In order to correct the PFGS for their detector response this quantity has to be known. Therefore the response matrices of all γ-ray detectors are simulated, in a energy range from 100 keV to 8 MeV with a 10 keV binning, by Geant4 [12]. In case of the HPGe detectors an additional procedure for the interpolation of the response matrix elements has been done to obtain a matrix elements in a finer energy step size of 2 keV. The detector resolution which is experimentally deduced from the energy calibration measurements is convoluted with the simulated response matrices afterwards. The matrix elements are normalized to the measured efficiencies. For the detector response correction the spectrum stripping method has been used [13]. The energy steps of the obtained emission spectra are equidistant with the same binning as the response matrices. The maximum energy limit is set to 5 MeV. The PFGS are extrapolated above 4.5 MeV for the $LaBr_3$ and above 2 MeV for the HPGe detectors. The minimum energy of the $LaBr_3$ detector was set to 100 keV and for the HPGe detectors to 150 keV due to the discriminator threshold behaviour. The final reponse corrected PFGS of our measurement are depicted in Fig. 5 in comparison to the measurement from Oberstedt et al. [14] and the calculation by the CGMF code [15], whose acquired PFGS also refers to the fission reaction ^{242}Pu(SF). The conditions and characteristics of these PFGS are shown in Table 2.

In our case the integral from the $LaBr_3$ spectrum with its lower energy threshold and lower amplitudes in comparison to the HPGe is about the same as the integrated HPGe spectrum which leads the the same multiplicity of $\overline{\nu}_\gamma \approx 8.1$. In comparison to the spectra from Oberstedt et al. and the CGMF calculation their values are lower than our measurement but agree for the most part of the spectrum within the errorbars to our results.

For the low energy region, as it is depicted in Fig. 5b), it can be seen that the PFGS of our $LaBr_3$ spectrum agrees quite well with the CGMF calculation. They differ from our HPGe spectrum and the result from Oberstedt et al. while these latter two spectra show a good agreement with each other. In the energy region for the PFGS which is shown in Fig. 5c) the CGMF calculation has

[4]The intensity should decrease exponentially in dependency of the time but cannot be seen here due to the short time window compared to the life time.

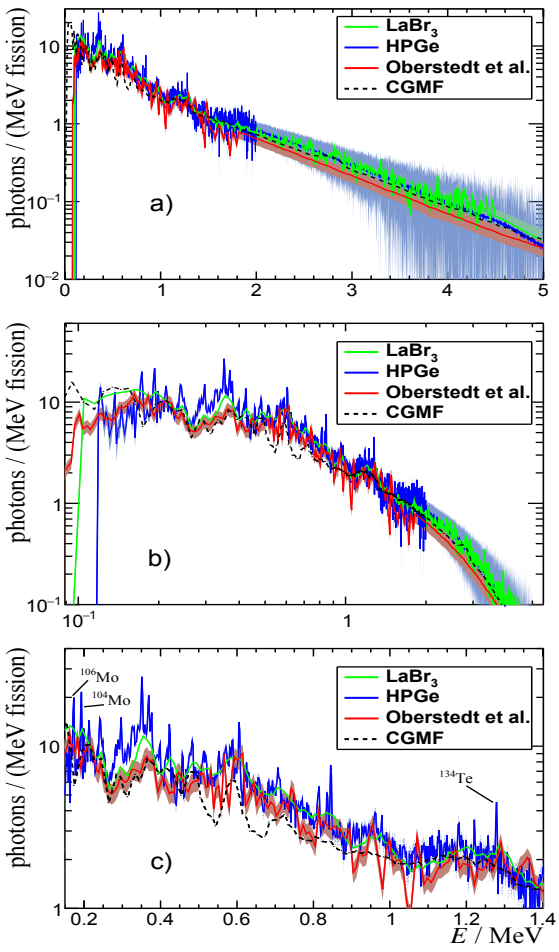

Figure 5. PFGS for ^{242}Pu from our measurement, averaged for all $LaBr_3$ and HPGe detectors, in comparison with the results from Oberstedt et.al [14] and the calculation from Stetcu [16] by the CGMF code [15]. The errorbars of the statistical uncertainties are depicted in a lighter color in comparison to its corresponding line color. In a) the PFGS with the entire energy range, in b) the PFGS in logarithmic energy scale are illustrated. The identified transitions from FF are pointed out in c) where a detail of the PFGS is shown.

significant lower values in comparison to the other measured spectra. The multiplicity of the spectrum of Oberstedt et al. and the CGMF calculation have approximately the same value of $\overline{\nu}_\gamma \approx 6.7$ due to the lower height of amplitude. This results also in a lower average total energy in comparison to our measurement whereas the mean energies agree better with each other[5].

The main contribution from the uncertainties of our PFGS characteristics result from systematic effects. These are efficiency- and response correction and the additional slow rise time trigger efficiency correction for the HPGe. The γ-ray energy from $(2^+ \rightarrow 0^+)$ quadrupole transitions of major FF ^{134}Te (1279 keV), ^{104}Mo (193 keV) ^{106}Mo (172 keV) could be identified (see Fig. 5c). Their life times are in the order of ns or less [11]. So it can be assumed that they completely contribute inside

[5]In case for the HPGe the mean energy is expected to be higher due to the higher threshold.

Table 2. Parameter of the PFGS from ^{242}Pu from this measurement in comparison with the results from Oberstedt et al. and the calculation by the CGMF code. The conditions low energy threshold E_{thr} and coincidence time window ΔT of the PFGS are shown with the characteristics average multiplicity per fission $\overline{\nu}_\gamma$, total energy $\overline{E}_\gamma$ and mean energy $\overline{\epsilon}_\gamma$.

	This work		Oberstedt et al. [14]	CGMF [16]
	$LaBr_3$	HPGe		
ΔT / ns	±3	±12	±10	±10
E_{thr} / keV	100	150	100	100
$\overline{\nu}_\gamma$	8.1±0.2	8.2±0.5	6.72±0.07	6.7
$\overline{E}_\gamma$ / MeV	6.8±0.2	6.9±0.4	5.66±0.06	5.87
$\overline{\epsilon}_\gamma$ / keV	839±10	870±20	843±12	870

the coincidence time window. For ^{134}Te the counts at the energy 1279 keV are enhanced by an additional contribution due to the ^{134m}Te deexcitiation which are occurring in the defined coincidence time window.

5 Conclusion

The PFGS measurement of ^{242}Pu was done with unprecedented statistics and for the first time HPGe detectors were used. Particularly for this type of detector a lot of effort has expended in terms of the the slow rise time rejection. The statistical uncertainty could be kept sufficiently low for very small energy steps which allows us to resolve E2 transitions from abundant FF. An isomeric state of the FF ^{134}Te (1279 keV) could be identified. Furthermore, the measured spectrum from the $LaBr_3$ detectors could be extended to 4.5 keV because of the high counting statistics. In comparison to the recent measurement from Oberstedt et al. and the CGMF calculation the spectral shape agrees well whereas the amplitudes differs from each other. With this setup, using $LaBr_3$ detectors and this type of fission chamber, also a neutron induced PFGS measurement is conceivable. The HPGe detectors are suited to study delayed γ-rays from isomeric states of FF, preferably from SF sources.

This work has been supported by the German Federal Ministry for Education and Science within the TRAKULA project (02NUK13A). The authors want to thank Andreas Hartman for the maintenance service of the HPGe detectors and Manfred Sobiella who made technical drawings of the MINICLUSTER which could be directly embedded in the Geant4 simulation. We want to thank A. and S. Oberstedt for their valuable advices about the PFGS measurement and also for the provision of their recent data of the PFGS of ^{242}Pu. Furthermore we want to thank I. Stetcu who made the model calculation for ^{242}Pu with the CGMF code.

References

[1] G. Rimpault, D. Bernaud, D. Blanchet, C. Vaglio-Gaudard, S. Ravaux and A. Santamarine Needs of Accurate Prompt- and delayed γ-spectrum und Multiplicity for Nuclear Reactor Designs. Phys.Proc. **31**, 3-12 (2012)

[2] WPEC. *The High Priority Request List for Nuclear Data (HPRL).* Working Party on International Evaluation Co-Operation, OECD / NEA (2011)

[3] R. Vandenbosch und J.R. Huizenga *Nuclear Fission* Academic Press Inc. (1973)

[4] T. Kögler, *Bestimmung des neutronen-induzierten Spaltquerschnitts von ^{242}Pu*. Dissertation, Technische Univeristät Dresden, Germany (2016)

[5] T. Kögler, R. Beyer, R. Hannaske, A.R. Junghans, R. Massarczyk, R. Schwengner and A. Wagner. *The nELBE (n, fis)*, Experiment, CERN-Proceedings-**2014-002**, 25-30 (2014)

[6] A. Vascon, J. Runke, N. Trautmann, B. Cremer, K. Eberhardt and C. Düllmann. Quantitative molecular plating of large-area ^{242}Pu targets with improved layer properties. Appl. Radiat. Isot. **95**, 36–43 (2015)

[7] D.W. Weißhaar, *MINIBALL: Ein neuartiges Gamma-Spektrometer mit ortsauflösenden Germaniumdetektoren* PhD thesis, Universität Köln (2003)

[8] H.G. Essel und N. Kurz. *GSI Multi-Branch System - Reference Manual, Version 5.1*. GSI, Gesellschaft für Schwerionenforschung mbH, Planckstraße 1, 64291 Darmstadt, Germany (2010)

[9] J. Adamczewski-Musch, M. Al-Turany, D. Bertini, H. G. Essel and S. Linev. *The Go4 Analysis Framework, Version 5* GSI, Gesellschaft für Schwerionenforschung mbH, Planckstraße 1, 64291 Darmstadt, Germany (2015)

[10] G.F. Knoll. *Radiation detection and measurement* John Wiley & Sons Inc., ISBN: 978-0-470-13148-0

[11] Brookhaven National Laboratory. *Nuclear Data Center* (2017)

[12] J. Allison, S. Agostinelli, K. Amako, J. Apostolakis, H. Araulo, P. Arce, M. Asai, D. Axen, S. Banerjee, G. Barrand, F. Behner, L. Bellagamba, J. Boudreau, L. Broglia, A. Brunengo, H. Burkhardt, S. Chauvie, J. Chuma, R. Chytracek, G. Cooperman et al. Geant 4- a simulation toolkit. Nucl. Instr. and Meth. A **506**, 250-303 (2003)

[13] A.K. Furr, E.L. Robinson and C. Robins. A Spectrum Stripping technique for qualitative activation analysis using monoenergetic gamma spectra. Nucl. Instr. and Meth. A **63**, 205-209 (1968)

[14] S. Oberstedt, A. Oberstedt, A. Gatera, A. Göök, F.-J. Hambsch, A. Moens, G. Sibbens, D. Vanleeuw und M. Vivaldi. Prompt fission γ-ray spectrum characteristics from ^{240}Pu(SF) and ^{242}Pu(SF) Phys. Rev. C **93** (2016)

[15] I. Stetcu, P. Talou, T. Kawano and M. Jandel. Properties of prompt-fission-γ-rays Phys. Rev. C **90** (2014)

[16] I. Stetcu. Private Communication (2017) Los Alamos National Laboratory (LANL)